Flame evolution in shock accelerated flow under different reactive gas mixture distributions

Yuejin Zhu[1,2], Longkun Gao[1], Kai Hong Luo[2], Jianfeng Pan[1], Zhenhua Pan[1], Penggang Zhang[1]
[1]*School of Energy and Power Engineering, Jiangsu University, Zhenjiang, 212013, China*
[2]*Department of Mechanical Engineering, University College London, Torrington Place, London, WC1E 7JE, UK*

1 Introduction

Flames in the reactive gas mixture subjected to the shock acceleration are usually unstable. This phenomenon is mainly due to the Richtmyer-Meshkov (RM) instability, and frequently occurs in industrial applications, such as the supersonic combustion propulsion [1] and industrial explosions [2]. Also it involves many complicated physics and chemical processes, which have not been fully understood.

A typical configuration to study the flame instability in shock accelerated flow is the shock-flame interaction, which has been widely investigated experimentally and numerically. Thomas et al. [3] experimentally studied the shock-flame interaction, and found that the RM instability was the main mechanism for the flame instability. Oran et al. [2,4] carried out a series of numerical studies on shock-flame interaction, and they found there would emerge hot spots and even detonation under a certain condition. They also found that the flame could be greatly disturbed and accelerated when a stronger reflected shock wave from right end wall impinged on the distorted flame again. In this case, a complex reactive shock bifurcation (RSB) structure (also called "strange wave" structure) may emerge via the shock wave-flame-boundary layer interactions. Moreover, in recent years, Zhu et al. [5,6] also studied the shock-flame interaction, and the influences of the initial parameters on the flame evolution were investigated in detail. Despite the extensive experimental and numerical studies in the past few decades, many issues concerning shock-flame interaction have not been resolved. Especially for practical situations, inhomogeneity in the reactive gas mixture can have a significant influence on the flame evolution, but few studies have been devoted to this topic.

Hence, in the present study, we numerically study the spherical flame evolution in the shock accelerated flow using the reactive Navier-Stokes equations under different reactive gas mixture distributions. The main aim is to investigate the influence of different reactive gas mixture gradients on the shock-flame interaction process.

2 Numerical method and setup

2.1 Numerical method

Correspondence to: k.luo@ucl.ac.uk; mike@ujs.edu.cn.

The two-dimensional axisymmetrical reactive Navier-Stokes equations coupled with one-step Arrhenius chemical reaction are utilized to simulate the shock-flame interaction, expressed as follows:

$$\frac{\partial U}{\partial t}+\frac{\partial F}{\partial x}+\frac{\partial G}{\partial y}+W=Q \tag{1}$$

where,

$$U=\begin{bmatrix}\rho\\ \rho u\\ \rho v\\ E\\ \rho S\end{bmatrix};\ F=\begin{bmatrix}\rho u\\ \rho u^2+p-\tau_{xx}\\ \rho uv-\tau_{yx}\\ (E+p)u-k\partial T/\partial x-u\tau_{xx}-v\tau_{yx}\\ \rho uS-D\rho\partial S/\partial x\end{bmatrix};\ G=\begin{bmatrix}\rho v\\ \rho uv-\tau_{xy}\\ \rho v^2+p-\tau_{yy}\\ (E+p)v-k\partial T/\partial y-u\tau_{xy}-v\tau_{yy}\\ \rho vS-D\rho\partial S/\partial y\end{bmatrix};\ W=\frac{v}{y}\begin{bmatrix}\rho\\ \rho u\\ \rho v\\ p+E\\ \rho S\end{bmatrix};\ Q=\begin{bmatrix}0\\ 0\\ 0\\ 0\\ -\rho\dot{\omega}\end{bmatrix}$$

ρ is the density, u and v are the velocities in the x and y directions, respectively, E is the total energy ($E=p/(\gamma-1)+0.5\rho\sum_{i=1}^{2}u_i^2+\rho qS$), p is the pressure, S is the mass fraction of the ambient reactive gas. τ_{xx}, τ_{xy}, τ_{yx} and τ_{yy} are the viscous stresses. In addition, W is the axisymmetric correction term, Q is the source term, and $\dot{\omega}$ is the chemical reaction speed which can be written as $\dot{\omega}=A\rho S\exp(-E_a/(RT))$, where A is the pre-exponential factor, E_a is the activation energy, R is the universal gas constant, and T is the temperature. All the related parameters in the above N-S equations can be referred in [5,6].

The splitting algorithm is adopted to solve the N-S equations. A global Lax-Friedrich's flux splitting combined with a ninth-order weighted essentially non-oscillatory (WENO) scheme [7] is used to discretize the spatial derivatives of inviscid fluxes. A tenth-order center difference scheme is employed for the viscous fluxes. Moreover, a third-order Runge-Kutta method is applied in time marching.

2.2 Computational setup

The computational setup is shown in Fig. 1, where the spherical flame with density of 0.01578 kg/m^3 is surrounded by the reactive gas mixture $C_2H_4/3O_2/4N_2$ with initial conditions of ρ_0=0.1615 kg/m^3, T_0=293 K at p_0=13.3 kpa. The incident shock wave initially moves from left to right to interact with the spherical flame, and reflects from the right end wall to interact with the distorted flame again. The computational domain is 170 mm × 38 mm, the uniform grid size is Δx=Δy=0.01 mm, and the resolution can fully correctly describe the flame development [2,5,6].

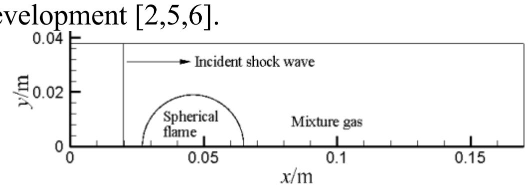

Figure 1 Schematic of the computational setup

Figure 2 gives the comparison between experimental Schlieren images [3] and computational density results at the selected time instants. Figures 2(a) and 2(b) firstly show the scenarios of incident shock wave (Mach number is 1.7) and spherical flame interaction. It can be found that the spherical flame distorts via RM instability behind the incident shock wave, and forms a pair of longitudinal symmetrical flame. Moreover, Figs. 2(c) and 2(d) correspond to the interaction of reflected shock wave with the distorted flame, and the flame expands drastically. A good qualitative agreement in distorted flame and shock wave evolution between the numerical simulation and experiment is obtained, which indicates the reliability of the numerical approach in the present study.

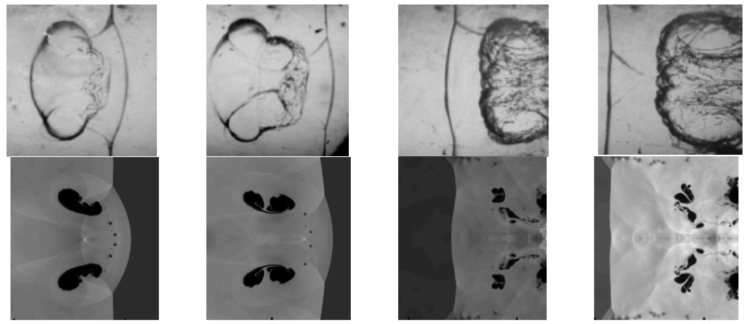

(a) t=143μs (b) t=194μs (c) t=443μs (d) t=494μs

Figure 2 Comparison between experimental Schlieren images[3] and computational density images at the selected time instants

3 Results and Discussions

Three cases with different initial reactive gas mixture distributions for the shock-flame interaction are investigated, with the same initial shock Mach number (Ma=2.51) in the present study. Specifically, the three different reactive gas mixture gradients are designed as follows:

$$S = 1 \ \ (case1);\ \ 1/[1+(2y/L_y)^2]\ \ (case2);\ \ [1+(2y/L_y)^2]/5\ \ (case3); \tag{2}$$

where L_y is the height of the computational domain in the y direction. The distributions of different reactive gas mixture gradients in the three cases are shown in Fig. 3. It can be found that case 1 corresponds to the uniform distribution of the reactive gas mixture, the distribution in case 2 has a negative gradient while the distribution in case 3 has a positive gradient.

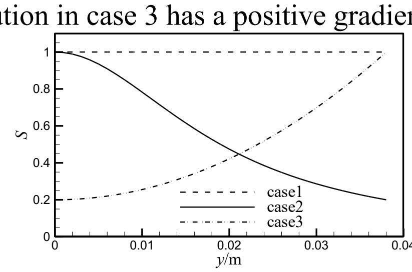

Figure 3 Reactive gas mixture distributions in the three different cases

Figure 4 presents the evolution of flame and waves in case 1, where the top half of each figure is the density distribution whilst the bottom half is the reactive gas mass distribution. Figures 4(a) and 4(b) correspond to the time instants when the incident shock wave has passed through the initial spherical flame. Because the acoustic impedance in the flame zone is smaller than that outside, the shock wave in the flame zone moves faster than the outside in Figs. 4(a) and 4(b). Meanwhile, the initial flame forms a pair of longitudinal symmetrical flames. When the reflected shock wave passes through the distorted flame in Fig. 4(c), the curving reflected shock wave collides in the vicinity of the symmetrical axis of the flow field to form a local high pressure zone. Then, the local hot spot in this high pressure zone will develop into detonation owing to the surrounding aboundant fresh reactive gas mixture and high temperature in Fig. 4(d). The detonation wave expands quickly and the fresh reactive gas mixture is also consumed fastly in Fig. 4(e). At t=231.2μs, the expanding detonation wave reflects from the top wall to form a new downward reflected shock wave RSW1 and a leftward Mach stem. Subsequently, the curved downward RSW1 collides in the vicinity of the symmetrical axis of the flow field again to form a new local high pressure zone and a new upward shock wave RSW2 in Figs. 4(g) and 4(h). Hence, a detonation emerges behind the leftward reflected shock wave due to the local high pressure zone in the vicinity of the symmetrical axis of the flow field. Moreover, the expanding detonation wave will turn into a planar detonation wave with triple points and transverse waves. To some extent, the revelation of the complicated waves in this case indicates the superiority of this high-order numerical method in present study.

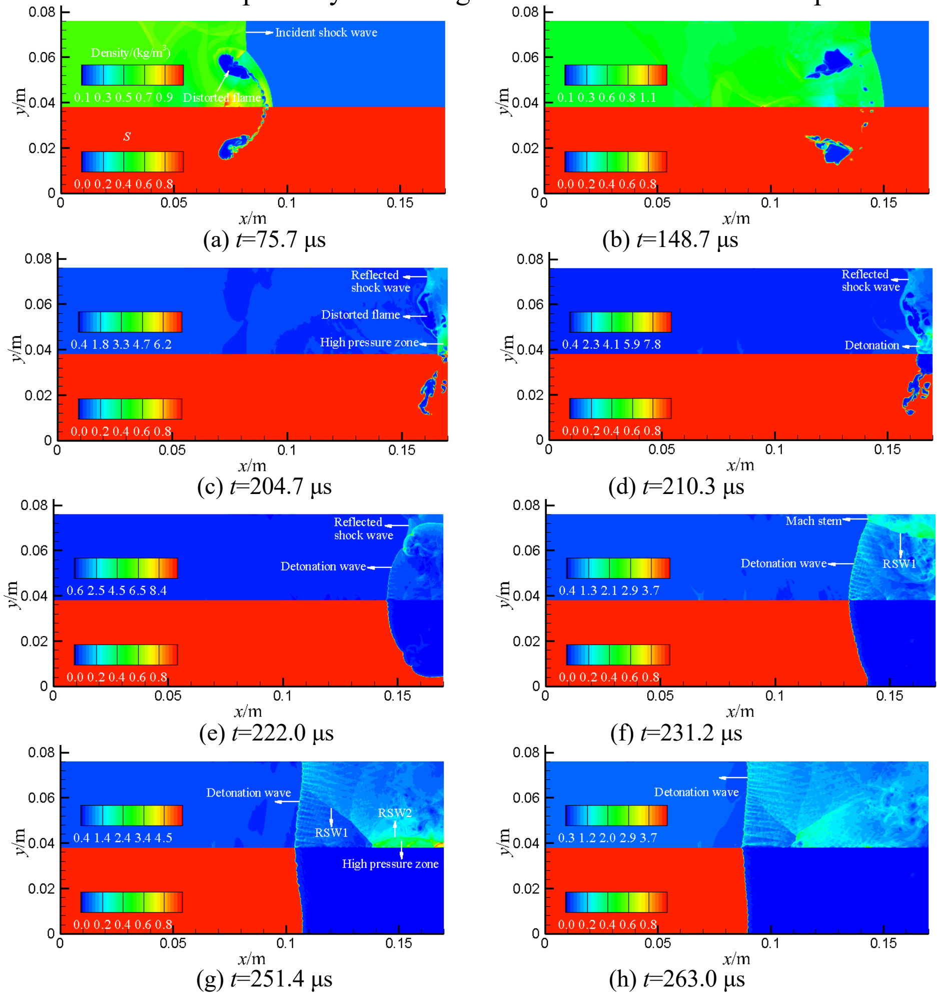

Figure 4 Computational density and reactive gas mixture mass images (Case 1)

For case 2 with negative reactive gas mixture gradient, Fig. 5 shows the evolution of flame and waves. A local high pressure zone is formed in Fig. 5(a) owing to the same reason as that for Fig. 4(c). Then, the surrounding waves of this local high pressure zone form a upward shock wave RSW1 and a leftward shock wave RSW2 in Figs. 5(b)-(d). Nevertheless, different from case 1, no detonation emerges in this case, and the reactive gas mixture in the local high pressure zone has not been consumed throughly compared with the results in Figs. 4(d) and 4(e). In the meantime, the distorted flame is further compressed by the reflected shock wave, and the area of the distorted flame and neighbouring low density zone decreases gradually. It implies that the chemical reaction speed is relatively slow in case 2, and more and more fresh reactive gas mixture has been entrained into the distorted flame zone. Moreover, it should be noted that a shock bifurcation emerges in the vincity of the top wall at the same time, and a similar structure called "strange wave" can be referred in [2,4]. A probable explanation is that the rightward flow velocity is relatively small in the boundary layer of the top wall compared with the flow velocity in the main flow, so the leftward reflected shock wave propagates in a reverse flow with a high velocity gradient, which will promote the reflected shock to emerge the reverse 'λ' shaped bifurcation in the vincity of the top wall. As time goes by, the original leftward reflected shock wave and the RSW2 wave are merged into a planar reflected shock wave, and the shock bifurcation is further developed in Figs. 5(e) and 5(f).

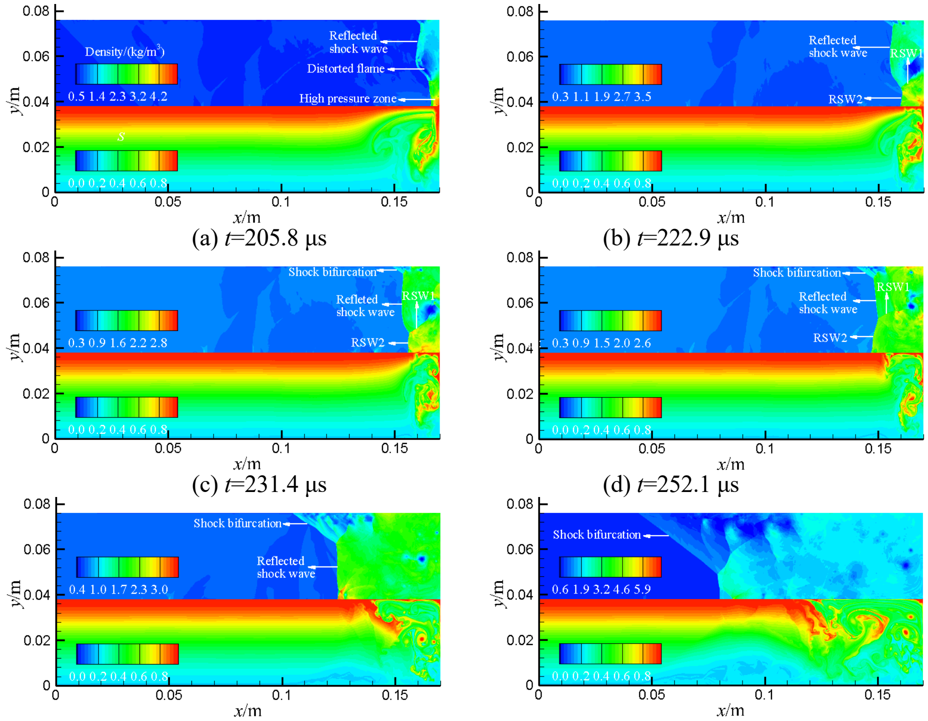

(a) t=205.8 μs (b) t=222.9 μs (c) t=231.4 μs (d) t=252.1 μs (e) t=340.5 μs (f) t=480.9 μs

Figure 5 Computational density and reactive gas mixture mass images (Case 2)

For case 3, Fig. 6 gives the evolution of flame and waves. A local high pressure zone is also formed in Fig. 6(a) owing to the same reason as those for Fig. 4(c) and Fig. 5(a). Then, similar upward shock wave RSW1, leftward shock wave RSW2 and the shock bifurcation can be found in Figs. 6(b) and 6(c). At t=330.4μs, the original leftward reflected shock wave and the RSW2 wave are merged into a planar reflected shock wave, and the shock bifurcation is further developed. Besides, the area of the distorted flame is still small at this time. However, the area of the distorted flame increases obviously in Fig. 6(e), which indicates that the chemical reaction speed increases quickly and more fresh reactive gas mixture has been involved in the combustion process. In Fig. 6(f), not only the original distorted flame expands greatly, but also a small wall flame emerges on the top wall. Hence, it is believed that a distinct increased heat release can be found at this time. Even so, there is no detonation in this case. But overall, the combustion intensity of case 3 has greatly enhanced compared with that of case 2.

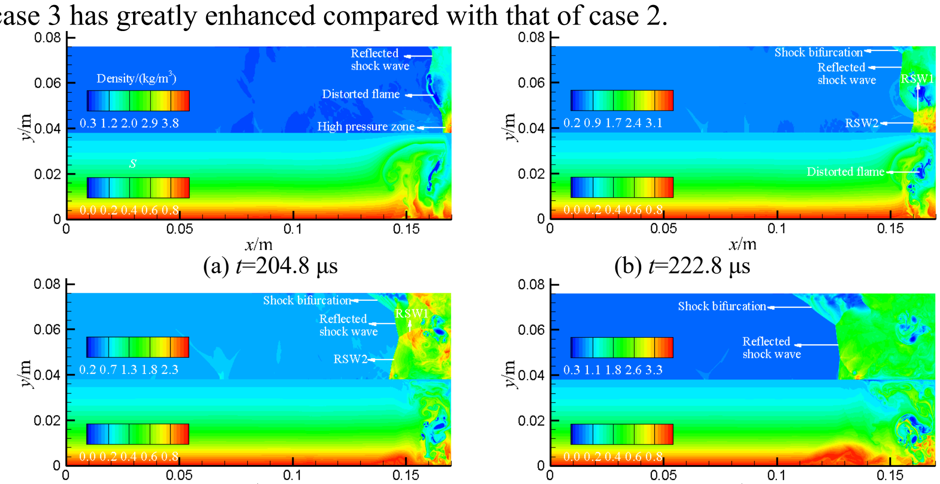

(a) t=204.8 μs (b) t=222.8 μs (c) t=263.0 μs (d) t=330.4 μs

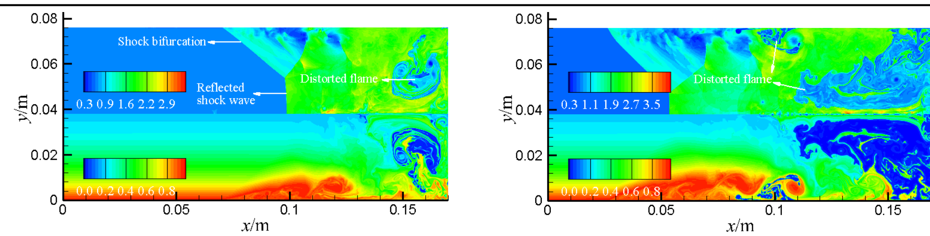

(e) t=410.6 μs (f) t=529.0 μs

Figure 6 Computational density and reactive gas mixture mass images (Case 3)

4 Conclusions

In present study, the spherical flame instability and acceleration induced by incident shock and its reflected waves are numerically studied with the same initial shock Mach number (Ma=2.51). In particular, the influences of different initial reactive gas mixture distributions on the shock-flame interaction are investigated. The main conclusions are summarized as follows: (1) A detonation emerges in case 1 with uniform reactive mixture gas distribution in present study, which can consume the fresh reactive gas mixture rapidly. (2) For case 2 with negative reactive gas gradient, no detonation emerges, and the area of the distorted flame decreases, thus the chemical reaction speed is relatively slow. Besides, a distinct shock bifurcation emerges from the vincity of the top wall owing to the leftward reflected shock wave propagates in a reverse flow with a high velocity gradient. (3) Different from case 2, the distorted flame expands quickly behind the leftward reflected shock wave in case 3 with positive reactive gas gradient, and the heat release also increases distinctly. (4) Overall, the different reactive gas mixture distributions greatly affect the flame evolution in shock accelerated flow, and the combustion intensities in case 2, case 3 and case 1 correspond to the weak, medium, and strong combustion, respectively.

Acknowledgements: This work was supported by the National Natural Science Fund of China (Grant Nos. 11872193, 91641113 and 11402102), the Jiangsu Overseas Visiting Scholar Program for University Prominent Young & Middle-aged Teachers and Presidents, and the Youth Talent Cultivation Plan of Jiangsu University.

References

[1] Yang J, Kubota T, Zukoski EE. (1994). Applications of shock-induced mixing to supersonic combustion. AIAA J. 31: 854.

[2] Oran ES, Gamezo VN. (2007). Origins of the deflagration-to-detonation transition in gas-phase combustion. Combust. Flame. 148: 4.

[3] Thomas GO, Bambrey R, Brown C. (2001). Experimental observations of flame acceleration and transition to detonation following shock-flame interaction. Combust. Theory Model. 5: 573.

[4] Gamezo VN, Oran ES, Khokhlov AM. (2005). Three-dimensional reactive shock bifurcations. Proc. Combust. Inst. 30: 1841.

[5] Zhu YJ, Dong G, Liu YX. (2013). Three-dimensional numerical simulations of spherical flame evolutions in shock and reshock accelerated flows. Combust. Sci. Technol. 185(10): 1415.

[6] Zhu YJ, Dong G, Liu YX, Fan BC, Jiang H. (2013). Effect of chemical reactivity on the detonation initiation in shock accelerated flow in a confined space. Acta Mechanica Sinica. 29(1): 54.

[7] Jiang GS, Shu CW. (1996). Efficient Implementation of Weighted ENO Schemes. J. Comput. Phys. 126: 202.